Jump reorientation of a molecular probe in the glass transition region of *o*-terphenyl

1996 J. Phys.: Condens. Matter 8 3795

(http://iopscience.iop.org/0953-8984/8/21/007)

J. Phys.: Condens. Matter **8** (1996) 3795–3809. Printed in the UK

Jump reorientation of a molecular probe in the glass transition region of *o*-terphenyl

L Andreozzi†§, F Cianflone†, C Donati‡§ and D Leporini†§‖

† Dipartimento di Fisica, Università di Pisa, Piazza Torricelli, 2, I-56100 Pisa, Italy
‡ Scuola Normale Superiore, Piazza dei Cavalieri, I-56100 Pisa, Italy

Received 4 December 1995

Abstract. The reorientation process of a molecular probe dissolved in the fragile glass former *o*-terphenyl is studied via electron spin-resonance spectroscopy. Owing to the good resolution of the ESR lineshape in the so-called slow-motion regime, we are able to discriminate between diffusive and jump rotations. In the region of the glass transition ($T_g - 31$ K $< T < T_g + 17$ K) the results are at variance with the diffusion models and are fairly well reproduced by assuming that the probe jumps with steps $\phi = 80^{\circ}{}^{+10^{\circ}}_{-5^{\circ}}$. The temperature dependence of the correlation time is well described, in the temperature range investigated, by a double Arrhenius law broken at T_g. The findings are compared with previous NMR, dielectric, fluorescence and molecular dynamics studies.

1. Introduction

Transport phenomena in highly viscous media and disordered solids are being actively studied [1–3]. It is well established that the microscopic dynamics is strictly related to the energy landscape, i.e. to the profile of the potential energy function Φ, depending in general on both the spatial location and the orientation of the particles [4]. One possibility for studying the complex topography of the hypersurface Φ is to dissolve probe molecules in the host medium. To capture the details of the rough energy landscape, one must resort to probes of sizes and shapes similar to those of the host molecules. It must be noted that, to study in more detail the distributions of the interaction potentials, which are a measure of the energy landscape [5], probe molecules which differ from the host ones could be needed.

Because of the roughness of the energy landscape and the highly branched character of the free-volume distribution, one expects that the dynamics of small probe molecules in disordered solids and highly viscous fluids will take place via jumps on short time intervals, whereas diffusive behaviour sets in on longer time-scales. The time at which the crossover between the two regimes takes place decreases on increasing the size of the probe molecule. It follows that the observation of jump motion should be regarded as evidence of good spatial resolution of the probe molecule, and the characterization of the related activation energy distribution as a measure of the roughness of the energy landscape explored during the time-scale of the experiment.

Electron spin-resonance spectroscopy (ESR) is a well established technique for studying microscopic single-particle dynamics [6]. It is often employed in the study of simple liquids,

§ INFM Udr Pisa.
‖ Corresponding author: FAX ++39 50 48277, e-mail: leporini@ipifidpt.difi.unipi.it.

0953-8984/96/213795+15$19.50

liquid crystals [7] and polymers [8], by dissolving in the host phase paramagnetic probe molecules—so-called *spin probes*—in very small amounts. In the limit of low concentration the resulting lineshape is found to be affected only by the rotational dynamics of the probe molecule. We are aware of only few ESR studies on supercooled fluids, with a very crude data analysis [9]. Several variants of the ESR experiment can be devised to explore the dynamic range of interest. Here, we will be concerned with the standard linear ESR, which covers approximately the dynamic range 10^{-12}–10^{-7} s. This range is particularly interesting since information about the single-particle dynamics on this scale is not easily accessed, and the importance of this time window has been recently emphasized by different theoretical approaches, dealing with the formation of amorphous phases via a glass transition [10, 11]. Further motivations for the present work may be drawn from the remark that the orientational disorder is usually overlooked with respect to the positional disorder, even when in ordinary amorphous systems both of them are obviously present. Even plastic crystals, e.g. fulleroids, adamantane, cyclohexanol and ethanol, exhibit glass-like orientationally disordered states in the presence of positional order [12].

The result of the present study, which extends a previous preliminary investigation [13], is twofold. Motivated by the limited number of examples in the literature [6, 7, 14], we provide new evidence about the sensitivity of the ESR technique for discriminating between different rotational models, even without resorting to deuterated spin probes. This sensitivity was not exploited in the limited set of ESR studies on supercooled fluids [9]. As a result, evidence that the jump rotations of molecular probes in a disordered model system on the nanosecond time-scale exist is provided, and they are characterized by studying the temperature dependence of the rotational correlation times and the size of the jump. The host and guest molecules have very similar molecular radii. The conclusions, although strictly referred to the guest molecules, show interesting correlations with recent molecular dynamics studies on the rotational dynamics of OTP.

2. Sensitivity of the ESR lineshape to the rotational model

Even while a number of methodologies are available to investigate the rotational motion, e.g. dielectric relaxation, nuclear magnetic resonance, neutron and light scattering, its complete characterization is rather difficult, and only partial information is usually obtained. The difficulty may be understood as follows. Having defined the orientation Ω in terms of Euler angles and assumed a stochastic picture, the singlet and conditional probabilities $P(\Omega_0)$, and $P(\Omega, t|\Omega_0)$ are the relevant quantities. The former yields the probability of having one molecule oriented at Ω_0, whereas the latter yields the probability of having the molecule oriented at Ω at time t, if initially it is at Ω_0. For a spherical molecule the conditional probability is expanded as [6, 15]

$$P(\Omega, t|\Omega_0) = \sum_{l,m,n} \frac{(2l+1)^2}{8\pi^2} D^{l*}_{m,n}(\Omega_0) D^{l}_{m,n}(\Omega) C_l(t) \tag{1}$$

where $D^l_{m,n}(\Omega)$ is one element of the Wigner rotation matrix with rank l. $C_l(t)$ is the correlation function of $D^l_{m,n}(\Omega)$. Equation (1) states that the knowledge of the conditional probability implies the knowledge of all of the correlation functions $C_l(t)$. This large amount of information is usually impossible to achieve. In many experiments the signal is proportional to ensemble averages of the form $\langle D^l_{0,0}\rangle$ with $l = 1$ or 2 and then, because of the well known orthogonality properties of the Wigner rotation matrix, they will depend only on $C_1(t)$ or $C_2(t)$. The case $l = 1$ is met in dielectric relaxation and infrared absorption,

whereas the case $l = 2$ is met in Raman spectroscopy, depolarization of fluorescence, and the Kerr effect [16].

The selection of only *one* term out of the expansion (1) is of valuable help for the purpose of interpreting the data, but limits the insight into the complete dynamical process.

In this respect the case of magnetic resonance deserves consideration in that, in contrast to what is the case for the above popular techniques, the molecular observable, i.e. the magnetization, does not 'stick' in the molecular frame. This implies that the molecular orientation Ω is not simply related to the *magnetization* orientation. Thus, the signal cannot be simply expressed in terms of ensemble averages $\langle D^l_{m,n} \rangle$, and several terms of equation (1) with different l-rank are expected to contribute [6]. Even if at first sight this feature seems to complicate the interpretation, it may in fact be used to improve the characterization of the rotational motion. Below, some theoretical considerations to clarify this point are offered.

In the ESR spectroscopy the static magnetic field H, defining the z-axis, splits the Zeeman levels of a paramagnetic sample. A small-amplitude, linearly polarized microwave field directed along the x-axis with frequency ν induces a dynamic magnetization perpendicular to H. The lineshape $L(H)$ is recorded by sweeping H around $H_0 = 2\pi\nu/\gamma$ (γ is the electron gyromagnetic factor). According to linear response theory, $L(H)$ may be expressed as the Laplace transform of a proper correlation function, namely [6]

$$L(H) = C\frac{\partial}{\partial H}\mathrm{Re}\int_0^\infty \langle M_x M_x(t)\rangle \mathrm{e}^{\mathrm{i}\gamma H t}\,\mathrm{d}t. \tag{2}$$

M_x is the x-component of the dynamic magnetization. The brackets indicate a proper thermal average, C is a constant, $\mathrm{Re}\{z\}$ is the real part of z, and $\mathrm{i}^2 = -1$.

Applications of the ESR spectroscopy to the study of the rotational motion of paramagnetic tracers ('spin probes') dissolved in liquids have been well known for some time [6]. The reorientation of spin probes broadens the resonance $L(H)$ because of the coupling between the spins and the molecular orientation via anisotropic Zeeman and hyperfine interactions [6]. When the molecule rotates, the coupling gives rise to fluctuating magnetic fields with amplitudes ranging between $\Delta H_{\min}$ and $\Delta H_{\max}$. They induce spin transitions which broaden the resonance. As an example, let us refer to the case of a spherical spin probe, and define τ_2 as the area under $C_2(t)$, i.e. τ_2 is the rotational correlation time. For $\tau_2 > 2\pi/(\gamma\,\Delta H_{\min}) = \tau_{\max}$ the ESR lineshape is a convolution of several narrow lines (spin packets) centred on particular values of the frozen-in fluctuating magnetic field. Any information in the lineshape on the dynamics of Ω is virtually lost. For $\tau_2 < 2\pi/(\gamma\,\Delta H_{\max}) = \tau_{\min}$ the orientation changes so rapidly that it is effectively averaged out. Again, this implies a loss of information on Ω, and in fact $L(H)$ depends only on the one-side Fourier transforms of $C_2(t)$. In the intermediate region $\tau_{\min} < \tau_2 < \tau_{\max}$ the orientation and the dynamic magnetization $M_\perp(t)$ fluctuate on comparable time-scales. One anticipates a good sensitivity to the details of the Ω fluctuations.

We have studied the sensitivity of $L(H)$ to the stochastic character of Ω by comparing the ESR lineshapes $L^J_\phi(H)$ and $L^D(H)$ evaluated under the assumptions that the spherical spin probe makes angular jumps of size ϕ [15] or reorients diffusively [16], respectively. Details on the numerical expansion of $L(H)$ in terms of continued fractions by using stochastic memory functions may be found elsewhere [17]. Here, we recall that the time evolution of $M_x(t)$ is governed by the Liouvillian $\mathcal{L}$, according to the equation of motion

$$\frac{\partial}{\partial t}M_x(t) = \mathcal{L}M_x(t) \tag{3}$$

where

$$\mathcal{L}A = \mathrm{i}[\mathcal{H}, A] + \Gamma A \tag{4}$$

where A is an operator, $\mathcal{H}$ is the spin Hamiltonian and $[A, B] = AB - BA$. The rotational dynamics of the spin probe is modelled via the Γ operator. For a spherically symmetric molecule rotating by instantaneous random jumps of fixed size ϕ after a mean residence time τ_0, a compact and fairly general expression of the Γ operator was derived [15]. In that case, according to the irreducible representation of the rotation group of rank l, the Γ operator is a multiple of the identity operator I_l, Γ_j, which is given by

$$\Gamma_j = \frac{1}{\tau_0}(\lambda_l I_l - 1) \qquad \lambda_l = \frac{1}{2l+1}\frac{\sin[(l+1/2)\phi]}{\sin(\phi/2)}. \tag{5}$$

In the limit where $\phi \ll 1$ the jump model reduces to the diffusion model, and Γ_j becomes

$$\Gamma_D = l(l+1)D \qquad D = \frac{\phi^2}{6\tau_0}. \tag{6}$$

For the diffusive and jump models the correlation time τ_2 reads [15]

$$\begin{aligned} \tau_2^D &= 1/(6D) \\ \tau_2^J &= \tau_0/[1 - \sin(5\phi/2)/(5\sin(\phi/2))]. \end{aligned} \tag{7}$$

To characterize the sensitivity of $L(H)$ to the stochastic character of Ω, a quantity s_ϕ is defined as

$$s_\phi(\tau_2) = \left\{ \lim_{\delta H \to \infty} \delta H^{-1} \int_{H_0 - \delta H/2}^{H_0 + \delta H/2} \left[L_\phi^J(H) - L^D(H) \right]^2 \, \mathrm{d}H \right\}^{1/2}. \tag{8}$$

$L_\phi^J(H)$ and $L^D(H)$ are both normalized to have unity maximum height. s_ϕ yields the fractional average deviation between the two lineshapes with respect to the maximum.

Figure 1 shows the dependence of the sensitivity s_{80° on τ_2 in the popular case of nitroxide spin probes also used in the present work [6]. s_{80° exhibits a peak between $\tau_{\min}$ and $\tau_{\max}$, as anticipated. It is apparent that over almost two decades in the region 5×10^{-9} s $< \tau < 5 \times 10^{-7}$ s the ESR spectroscopy is expected to discriminate effectively between different models of rotational motion. The maximum sensitivity is larger than 8%. Further analysis of the model dependence of the ESR lineshape is given in figure 2 where $L_\phi^J(H)$ and $L^D(H)$ are compared for different values of the jump angle ϕ and $\tau_2 = 2.8 \times 10^{-8}$ s. If $\phi > 10^\circ$, differences in the lineshapes calculated assuming either the diffusion or the jump model are clearly visible.

3. Experimental details

Samples were prepared by dissolving TEMPO radical (2, 2, 6, 6 tetramethylpiperidin-1-oxyl, 98% Aldrich) in as-received OTP (99% Aldrich, $T_g = 243$ K) in a concentration of 10^{-3} mol l^{-1}. After further dilution of TEMPO no change in the ESR lineshape was detected. The molecular structures of TEMPO and OTP molecules are shown in figure 3. Their average Van der Waals radii r are comparable, being $r_{OTP} = 0.37$ nm [18] and $r_{TEMPO} \approx r_{TEMPONE} = 0.33$ nm [19]. The magnetic parameters of TEMPO used in the data analysis were obtained by careful numerical simulation of the powder ESR spectrum of TEMPO. The samples were degassed with nitrogen flow for twenty minutes and then sealed in standard quartz tubes in nitrogen atmosphere. To prevent crystallization, the sample was preliminarily annealed at a temperature $T = 350$ K for about 15 min and then quenched at the lowest temperature of interest. All data were recorded on heating. After each temperature step an annealing period of 20 min was ensured. During the equilibration no appreciable changes in the ESR lineshape were observed. ESR measurements were carried

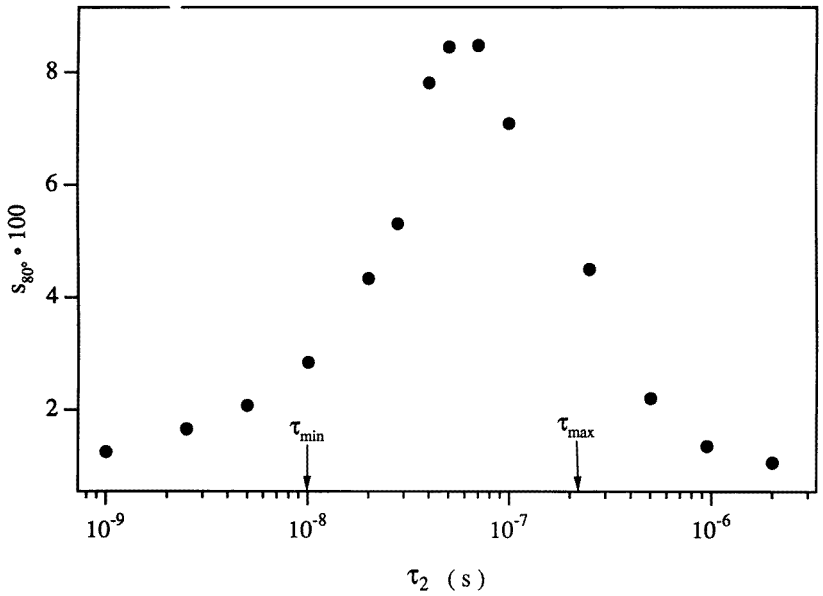

Figure 1. A plot of the sensitivity s_{80° versus the correlation time τ_2 for a nitroxide spin probe. The magnetic parameters used in the calculations are (x-axis parallel to the N–O bond, z-axis parallel to the 2pπ orbital of the nitrogen, y-axis perpendicular to the other two): $g_{xx} = 2.0086$, $g_{yy} = 2.0058$, $g_{zz} = 2.0019$, $A_{xx} = 9$ G, $A_{yy} = 6$ G, $A_{zz} = 33.85$ G. $L^J_{80^\circ}(H)$ and $L^D(H)$ were convoluted with a gaussian whose width is $w_J = 1$ G and $w_D = 1$ G, respectively.

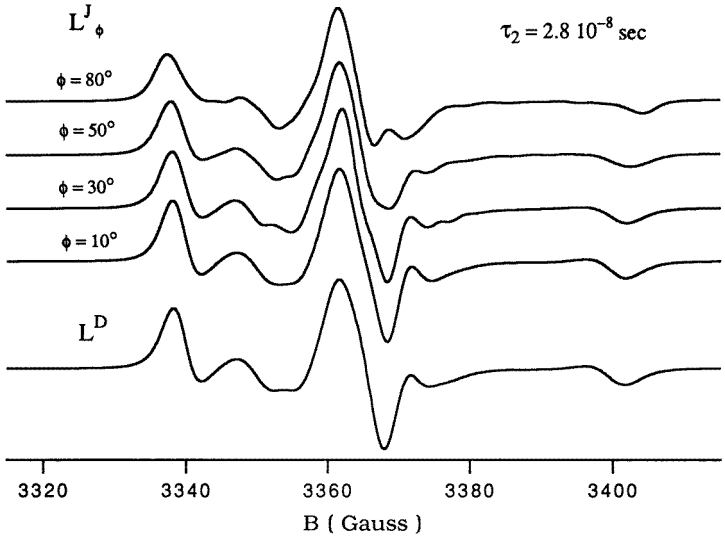

Figure 2. A comparison of $L^J_\phi(H)$ and $L^D(H)$ for different values of the jump angle ϕ. The magnetic parameters are as for figure 1. The gaussian convolution width is $w_J = w_D = 1$ G.

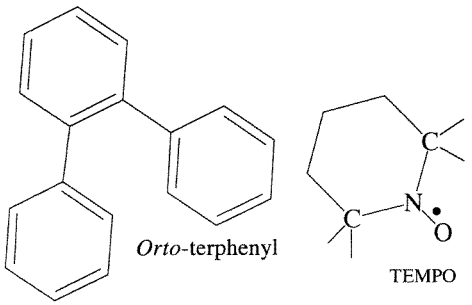

Figure 3. The structures of the molecules of OTP and TEMPO.

out by using a Bruker spectrometer ER200D equipped with an X-band bridge supplying at 0 dB and 200 mW, a NMR gaussmeter ER035M, and a gas-flow variable-temperature unit. All data were recorded on a Macintosh computer and analysed off-line.

4. Results and discussion

In figure 4 the experimental lineshapes are compared with the theoretical predictions of the jump and diffusion models $L^J_\phi(\omega)$ and $L^D(\omega)$, respectively. To account for the residual broadening, both $L^J_\phi(\omega)$ and $L^D(\omega)$ have been convoluted with gaussians having widths w_J and w_D, respectively. The gaussian width is only slightly temperature dependent. In the calculation of $L^J_\phi(\omega)$ the only adjustable parameters are the residence time τ and the jump size ϕ. The theory was fitted to the experimental curves by adjusting both parameters. The angle was set to $\phi = 80^{\circ\,+10^\circ}_{\;-5^\circ}$ at the lowest temperature investigated ($T_g - 31$ K). No meaningful temperature dependence of the jump size was observed in the temperature range investigated. The error on ϕ is set by the finite sensitivity of $L^J_\phi(\omega)$ to the jump size. We carefully checked that outside of the above range of ϕ-values $L^J_\phi(\omega)$ disagrees appreciably with the experiment. In the calculation of $L^D(\omega)$ only the diffusion constant D has been adjusted. In agreement with previous studies on non-polar structureless liquids the best fit for the diffusion model is achieved by assuming a spherical diffusion tensor for TEMPO [19]. It is apparent that the experimental data agree well with the predictions of the jump model $L^J_{80^\circ}(\omega)$ over a range of about 50 degrees around the glass transition. The agreement is virtually perfect at the lowest temperature (figure 4). At higher temperatures ($T > T_g$) some deviations between the experimental lineshape and $L^J_{80^\circ}(\omega)$ become apparent. The deviations cannot be reduced appreciably by extending the jump model, so the size of the jump ϕ is distributed, according to a rectangular distribution of jump steps $p(\phi)$ [15]. The limited effect of this extension has been already noticed in the past [20]. Our results compare well with previous ESR studies by Freed and collaborators on the rotational motion of PD-Tempone, which is virtually identical to TEMPO, in toluene-d_8 and 85% glycerol-d_3-D_2O [19]. There, an isotropic jump model with an rms jump angle of about 50° was found to be in very good agreement with the experiment for temperatures corresponding to $\tau_2 = 1.0 \times 10^{-8}$ s and $\tau_2 = 1.5 \times 10^{-8}$ s, respectively.

Figure 5 shows a more detailed comparison between the prediction of the jump model and the experimental data. It is seen that the jump model captures details of the ESR lineshape rather better than the diffusion model, but needs to be improved above T_g.

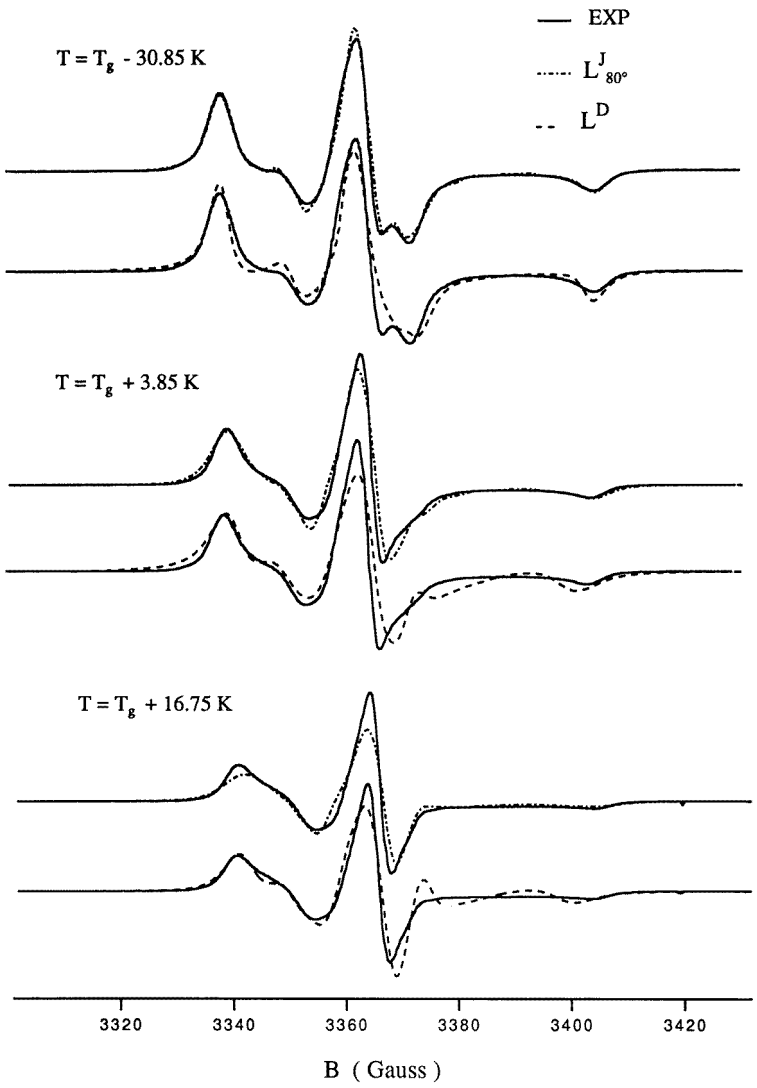

Figure 4. A comparison between the experimental ESR lineshape and best fits according to the jump and diffusion models, $L^J_{80°}(H)$ and $L^D(H)$ respectively, at different temperatures. The magnetic parameters are as for figure 1. Top: $\tau_2^D = \tau_2^J = 2.8 \times 10^{-8}$ s, $w_J = w_D = 1$ G; middle: $\tau_2^D = \tau_2^J = 1.5 \times 10^{-8}$ s, $w_J = w_D = 1$ G; bottom: $\tau_2^D = \tau_2^J = 9.15 \times 10^{-9}$ s, $w_J = 0.75$ G, $w_D = 0.7$ G.

Further quantitative comparison between the two models was made by defining

$$d^J = \left\{ \lim_{\delta H \to \infty} \delta H^{-1} \int_{H_0 - \delta H/2}^{H_0 + \delta H/2} \left[L^J_\phi(H) - L(H) \right]^2 \, \mathrm{d}H \right\}^{1/2} \tag{9a}$$

$$d^D = \left\{ \lim_{\delta H \to \infty} \delta H^{-1} \int_{H_0 - \delta H/2}^{H_0 + \delta H/2} \left[L^D(H) - L(H) \right]^2 \, \mathrm{d}H \right\}^{1/2} . \tag{9b}$$

$L^J_\phi(H)$ and $L^D(H)$ are the best-fit curves of the experimental ESR lineshape $L(H)$. $L^J_\phi(H)$,

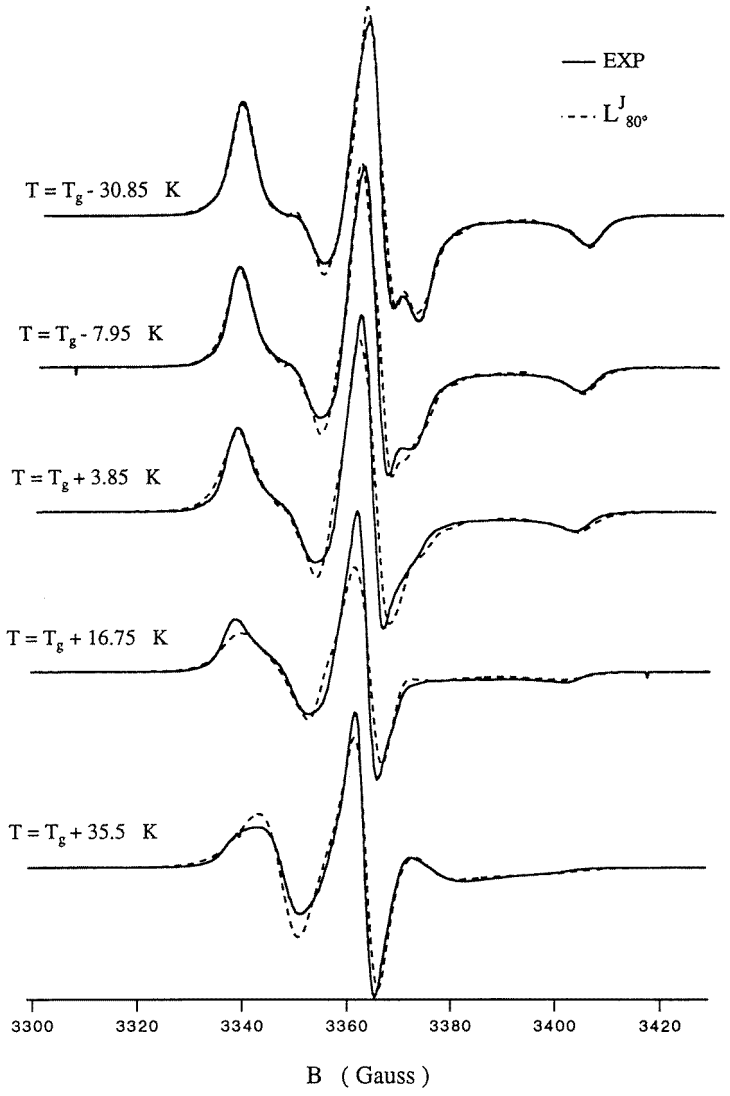

Figure 5. A comparison between the experimental ESR lineshape and best fit according to the jump model for different temperatures. The magnetic parameters are as for figure 1. From the top: $\tau_2^J = 2.8\times10^{-8}$ s, $w_J = 1$ G; $\tau_2^J = 2.2\times10^{-8}$ s, $w_J = 1$ G; $\tau_2^J = 1.5\times10^{-8}$ s, $w_J = 1$ G. $\tau_2^J = 9.2\times10^{-9}$ s, $w_J = 0.75$ G; and $\tau_2^J = 5.6\times10^{-9}$ s, $w_J = 0.6$ G.

L^D and $L(H)$ are normalized to have unity maximum height. Similarly to the sensitivity defined by equation (8), d^J and d^D yield the fractional average deviation with respect to the maximum height. Table 1 lists d^J and d^D for the five cases of figure 5. The correlation times τ_2, as derived from the fitting procedure, are also included. By inspecting figure 1, it is seen that the values of τ_2 cover the left wing of the curve showing the sensitivity of the ESR lineshape to the rotational model. Table 1 confirms that the jump model always provides a better fit than the diffusional model. At lower temperatures, i.e. in the range of maximal sensitivity (see figure 1), the jump model deviations are up to four times smaller

Table 1. Fractional deviations and best-fit values of the correlation times according to the jump and the diffusional models.

T (K)	d^J	d^D	τ_2^J (ns)	τ_2^D (ns)
212.15	0.019	0.076	28	28
235.05	0.025	0.066	22	20
246.85	0.030	0.074	15	15
259.75	0.037	0.047	9.2	9.2
278.45	0.028	0.036	5.4	5.0

than the diffusional model ones. At higher temperatures d^J increases and becomes closer to d^D. However, even if the sensitivity of the ESR lineshape to the rotational model s_{80° is reduced, it is found that d^D exceeds d^J by about 30%.

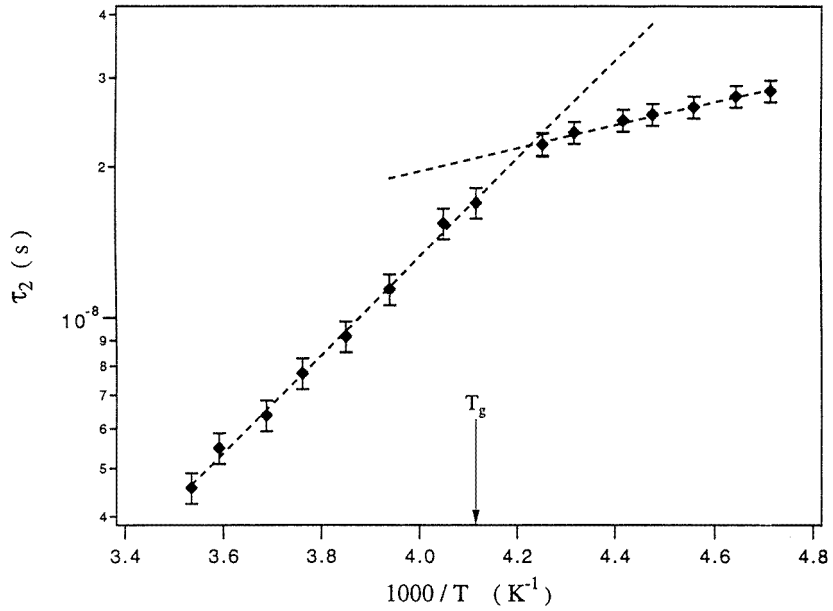

Figure 6. The temperature dependence of τ_2^J in the glass transition region. The data were collected on heating. The dashed lines are the best fits according to the Arrhenius law $\tau_2(T) = f^{-1}\exp(E/RT)$. For $T < T_g$, $f = (4.16 \pm 0.4) \times 10^8$ Hz, $E = 4.37 \pm 0.4$ kJ mol^{-1}; for $T > T_g$, $f = (1.26 \pm 0.1) \times 10^{12}$ Hz, $E = 18.7 \pm 1$ kJ mol^{-1}.

The numerical simulations of the ESR lineshape carried out according to the jump model depend on the residence time τ_0 and the jump angle ϕ. Their best-fit values have been used to calculate the correlation time τ_2 via equation (2). Figure 6 shows the temperature dependence of τ_2 in the glass transition region observed on heating. It is well described by a double Arrhenius law broken at a temperature $T_b = 238 \pm 2$ K close to the calorimetric value $T_g = 243$ K. The offset between T_b and the calorimetric value T_g is expected, since the average structural relaxation time at T_g is about 100 s—i.e. shorter than the equilibration period (20 min). The increase in the activation energy on heating across T_g is interpreted via the following simple argument. Below T_g no structural change takes place and the reorientation of TEMPO occurs via activated jumps in a fixed structure. Above T_g the

structure becomes more open with a finite activation energy which contributes to the *total* activation energy needed for each rotation. This picture is consistent with the observed increase in the attempt frequency f (i.e. the inverse of the prefactor in the Arrhenius law for τ_2) an increasing the temperature. In the glass region $f = 4.2 \times 10^8$ Hz, whereas in the supercooled region $f = 1.3 \times 10^{12}$ Hz. The former suggests that TEMPO rotations are hindered in the OTP glass, whereas the latter compares well with the inverse of the rotational correlation times usually measured in low-viscosity fluids. Our findings confirm that the glass transition can be revealed by changes in slope, or discontinuities, in virtually any measurable property that depends on liquid structure. Examples can be drawn from dielectric relaxation [21], tracer diffusion [22], NMR [23], rotational dynamics [24] and conductivity [25] where a change from an Arrhenius to a Vogel–Fulcher (VF) law is usually observed on crossing T_g. In the present study an Arrhenius law rather than the customary VF law is observed for $T > T_g$. Extending the study to higher temperatures above T_g does not alter this conclusion. Instead, a more complex temperature dependence of τ_2 is observed which will be discussed elsewhere [26].

By inspection of figure 6 it is seen that the correlation time $\tau_2 \equiv 10^{-8}$ s at T_g, and follows an Arrhenius law with a small activation energy of about 20 kJ mol^{-1} for $T > T_g$. In this respect it must be noted that Rössler and co-workers observed via ^{2}H-NMR that small guest molecules with high symmetry, like benzene, experience in tricresyl phosphate (TCP) both a slow overall reorientation which is well coupled to the structural relaxation of TCP and fast jump rotations. As in the present case, the latter exhibits a double Arrhenius temperature dependence broken at T_g with activation rates of the order of 20 kJ mol^{-1} for $T > T_g$ [27]. The conclusion that small molecules dissolved in supercooled OTP may undergo both slow (α-) and fast (β-) rotations was also reached via dielectric relaxation by Williams and Hains [28] and Shears and Williams [29]. The α-rotation is well coupled to the cooperative rearrangement of OTP. Contrastingly, the β-rotations were expected in the microwave region [28] and ascribed to either restricted rotations, relaxation in a temporary barrier system provided by adjacent OTP molecules, or the dipole sometimes finding itself in environments which allow easy reorientation [29]. For the highly symmetric camphor molecule it was found that, even if the loss curve peak was located at $\log_{10}(f_m/\mathrm{Hz}) = 2.70$ at $T = 260.1$ K, the dipole moment was reduced by more than one third by the β-process [28]. Comparable or stronger averaging was measured in less symmetric molecules like 1-chloro-naphthalene [28] and benzophenone [29]. For larger molecules, like phthalic anhydride and anthrone [28], only α-rotations were detected.

Relevant to this discussion is the study of the rotational motion of a number of solutes in OTP by Cicerone and collaborators via time-resolved optical spectroscopy [30]. For large molecules like anthracene, tetracene, and rubrene, slow reorientations well coupled to supercooled OTP were observed. In particular, the authors exclude the possibility of other, faster rotations for the very large and flat rubrene molecule but, more interestingly, for the smaller anthracene molecule allow the possibility that up to half of the correlation function decay occurred during the dead time of their photobleaching apparatus (1 ms or longer).

In conclusion, we think that the rotational motion of TEMPO detected by ESR is strictly related to the fast motions claimed in molecules like benzene, benzophenone, camphor, 1-chloro-naphthalene and anthracene, whose sizes are comparable to or larger than that of TEMPO. Slower reorientations of TEMPO cannot be excluded. However, they should be in the region of 10^{-3} s or longer in the temperature region investigated, and therefore cannot be detected in our ESR experiment ($\tau_2 < 5 \times 10^{-7}$ s).

As noted above, the β-rotations of small solutes in OTP are rather effective in averaging the dipole moment in dielectric relaxation. That is at odds with the hypothesis that for

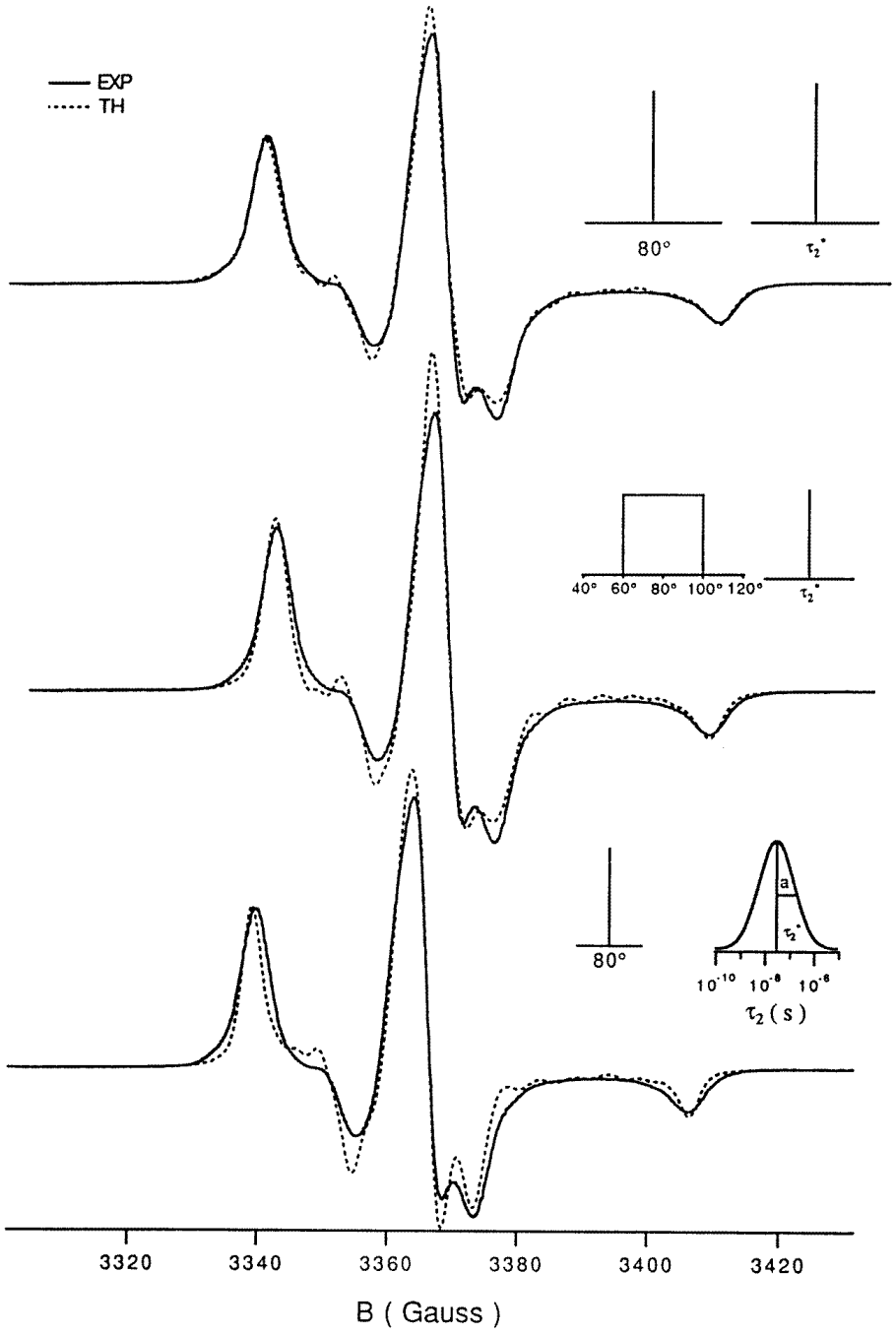

Figure 7. A comparison of three rotational models with the experimental ESR lineshape at $T = T_g - 30.85$ K. Top: single jump size, single correlation time. Middle: heterogeneous, flat distribution of jump size, single correlation time. Bottom: single jump size, log–gauss distribution of correlation times. $\tau_2^* = 2.8 \times 10^{-8}$ s. $a = 0.833$.

temperatures which are comparable to or larger than T_g fast rotations occur through a small libration angle $\Delta\Theta$. For example, at $T_g + 15$ K, for 1-chloro-naphthalene and camphor one estimates from [28] $\Delta\Theta \approx 100^\circ$. The present study agrees with the above findings for the following reasons.

(1) In the presence of highly restricted rotations no motional narrowing of the ESR lineshape should be observed [31]. Instead, figures 4 and 5 prove that the ESR lineshape is motionally narrowed. Restricted rotations ($\Delta\Theta = 10^\circ$) of TEMPOL, which is very similar to TEMPO, have been observed in polystyrene at $T_g - 120$ K corresponding to about 40 K below the temperature at which the ESR lineshape starts to be motionally narrowed [31].

(2) On lowering the temperature, $\Delta\Theta$ should decrease, leading to increasing discrepancies between the experimental ESR curve and the theory, which assumes isotropic reorientations. Instead, the theory fits well to the experiment at lower temperatures (figures 4 and 5). Note that at the lowest temperature, the sensitivity of the ESR lineshape to the geometry of the rotations is close to the maximum (figure 1).

Isotropic rotations are expected in highly symmetric molecules like tetramethylsilane and adamantane [27]. TEMPO is only approximately spherical in shape. Nonetheless, neither the good agreement between theory and experiment especially at the lowest temperatures (figures 4 and 5; see also figure 7 discussed below), nor the arguments presented above, nor previous ESR results [19] support the view that in the temperature range investigated the TEMPO rotations are highly restricted on the ESR time-scale. However, in the present and previous ESR studies [19], quantitative comparisons with models for anisotropic rotations are lacking due to numerical difficulties. Therefore, and also in view of other studies [28, 29, 31], we are cautious about concluding in favour of the full isotropic character of the fast rotations of TEMPO discovered by ESR. Only investigations on longer time-scales, e.g. via NMR or dielectric relaxation, could be decisive as regards assessing the isotropic character of the β-rotation detected by ESR.

Our data analysis describes the rotational motion of TEMPO via a single correlation time τ_2 and a single jump size ϕ. These assumptions have been checked at $T = T_g - 30.85$ K, where the model sensitivity of the ESR lineshape is at its maximum. In figure 7 our model is compared with models assuming heterogeneous distributions of jump sizes and correlation times. It is found that even relatively narrow distributions lower the quality of the fit at that temperature. We conclude that, even if TEMPO is approximately spherical and the jump sizes are presumed to be distributed, the width of such a distribution is not large. This finding is not unexpected. In fact, if a single jump size ϕ is assumed, a limited uncertainty on the best-fit value is found ($\phi = 80^{\circ\,+10^\circ}_{\;-5^\circ}$ at $T = T_g - 30.85$ K). On the other hand, the absence of a wide distribution of correlation times may be understood as being due to the poor coupling between OTP and the fast reorientations of TEMPO [32]. Instead, in the presence of stronger coupling with the structural relaxation—as in the case of the α-reorientation of solutes dissolved in TCP—a non-exponential correlation loss is found [27].

The observation of jump rotations of a TEMPO molecule does not imply necessarily that an OTP molecule does the same. Anyway, TEMPO and OTP have similar size and it is tempting to compare the two behaviours. This is also motivated by the remark that, despite of the fact that OTP is probably the most thoroughly investigated model system in glass transition studies, the nature of its rotational motion is still an open question. Several years ago Beevers *et al* found that in the temperature range from $T_g + 7$ K to $T_g + 27$ K rotational correlation times of OTP drawn from dielectric relaxation ($l = 1$) and Kerr effect ($l = 2$) measurements were equal [20]. Their observations are at variance with the hypothesis

of rotational diffusion, and call for a model of rotational motion involving large angular jumps. The authors were not able to give a quantitative estimate of the jumps. In a series of studies on OTP via ^{2}H-NMR, Sillescu and collaborators concluded that OTP does not show any internal dynamics on the microscopic or mesoscopic time-scale [18, 33]. They found that at $T = T_g + 9$ K and on the scale of evolution times τ_1 of tens of microseconds, the reorientation of OTP is described by a distribution of rotational jump angles centred at $\approx 10^\circ$ [34]. However, larger jump angles cannot be excluded for evolution times $\tau_1 < 5$ μs (ϕ comparable to or larger than 35°; see figure 3 of [34]). Very recently, a detailed molecular dynamics study of relaxation in OTP was carried out by Lewis and Wahnström [35, 36]. The study addresses the rotational dynamics of OTP. During an observation time of 1 ns, the nature of the translation-free orientational motion covers a large spectrum of situations, grouped roughly into three classes at $T = T_g + 23$ K. Approximately two thirds of molecules exhibit only small-amplitude librations around their equilibrium orientation. The rest (one third) are found to undergo some type of reorientational motion, mainly jumps of about 90° or—rarer—almost diffusive motion [35]. The observation of jumps of about 90° (see also figure 11 in [36]) could be related to the model, since a bond angle of 75° was used [37].

At $T = T_g + 23$ K, the rotational correlation time of TEMPO ($\tau_2 = 6 \times 10^{-9}$ s) falls in the time window studied by Lewis and Wahnström and it is found that TEMPO rotates by jumps as wide as $\phi = 80^{\circ\,+10^\circ}_{\;-5^\circ}$, i.e. very close to the OTP jump size. The TEMPO and OTP molecules have similar radii but different shapes and, in principle, different ways of rotating cannot be excluded. However, one may speculate that the OTP and the TEMPO molecules will exhibit similar reorientation dynamics at short times in the available free volume.

5. Conclusions

The role of the rotational degrees of freedom in supercooled fluids is not completely understood. ESR spectroscopy is particularly well suited to the study of rotational dynamics over a wide range of correlation times. Surprisingly, only few studies concerning molecular glass formers are known, providing very crude data analysis [9]. To demonstrate the possibility of ESR, the present work has discussed the sensitivity of the lineshape to different models of rotational dynamics. The sensitivity is particularly enhanced in the so-called slow-motion regime, covering approximately the range of correlation times 5×10^{-9} s $< \tau_2 < 5 \times 10^{-7}$ s (see figure 1). The rotational motion of probe molecules in the glass transition region of OTP has been characterized without resorting to predeuterated materials [6, 7]. At $T_g - 31$ K the experimental evidence is in favour of jump rotations with steps of $\phi = 80^{\circ\,+10^\circ}_{\;-5^\circ}$. In the temperature range from $T_g - 31$ K to $T_g + 16$ K, ϕ is virtually constant. At higher temperatures small deviations call for an extension of the model. The presence of highly restricted rotations is not supported by the present study. Nonetheless, we are cautious about concluding in favour of the full isotropic character of the fast rotations of TEMPO discovered by ESR. The jump size and the correlation time of TEMPO are found to be not widely distributed. The absence of a wide distribution of correlation times is ascribed to the poor coupling between OTP and the fast β-reorientations of TEMPO [32].

The temperature dependence of the rotational correlation time of TEMPO is well fitted by a double Arrhenius law with a knee close to T_g in agreement with other ^{2}H-NMR studies of molecular probes in fragile glass formers [27]. Possible correlations between the rotation mechanisms of the guest and host molecules have been discussed in the light of recent results from molecular dynamics [34–36].

Acknowledgments

One of the authors (DL) thanks Professors L Lewis and G Wahnström for helpful comments and unpublished details about their work, Professor G P Johari for discussions about relaxation in supercooled fluids, Professor Dr H W Spiess for preprints, and Professor Dr E Rössler and Professor Dr H Sillescu for reprints. Financial support from the Istituto Nazionale di Fisica della Materia is also gratefully acknowledged.

References

[1] Jäckle J 1986 *Rep. Prog. Phys.* **49** 171
[2] Richert R and Blumen A (ed) 1994 *Disorder Effects on Relaxational Processes* (Berlin: Springer)
[3] See
1995 *Science* **267** March issue
[4] Stillinger F H 1995 *Science* **267** 1935
Goldstein M 1969 *J. Chem. Phys.* **51** 3728
[5] See
Rössler E and Taupitz M 1986 in [1] p 361
[6] Slichter C P 1992 *Principles of Magnetic Resonance* (Berlin: Springer)
Muus L T and Atkins P W (ed) 1972 *Electron Spin Relaxation in Liquids* (New York: Plenum)
Freed J H 1976 *Spin Labeling: Theory and Applications* ed L J Berliner (New York: Academic)
[7] Freed J H 1987 *Rotational Dynamics of Small and Macromolecules (Springer Lecture Notes in Physics 293)* ed T Dorfmüler and R Pecora (Berlin: Springer)
[8] Andreozzi L, Giordano M, Leporini D, Martinelli M and Pardi L 1991 *Phys. Lett.* **160A** 309
Andreozzi L, Fontana M P, Francia F, Giordano M, Leporini D and Rateo M 1994 *Proc. 2nd Int. Discussion Mtg on Relaxations in Complex Systems* ed K L Ngai, E Riande and G B Wright; *J. Non-Cryst. Solids* **172–174** 943
Andreozzi L, Chiellini E, Giordano M and Leporini D 1995 *Mol. Cryst. Liq. Cryst.* **266** 73
[9] Spielberg J and Gelerinter E 1982 *J. Chem. Phys.* **77** 2159
Ohta N and Kuwata K 1985 *J. Chem. Phys.* **82** 3420
[10] Ngai K 1986 *Rep. Prog. Phys.* **49** 171
[11] Götze W 1991 *Liquids, Freezing and the Glass Transition* ed J-P Hansen, D Levesque and J Zinn-Justin (Amsterdam: North-Holland)
[12] Johari G P 1992 *J. Chim. Phys.* **89** 2073
[13] Andreozzi L, Donati C, Leporini D and Giordano M 1994 *Proc. 1st Int. Conf. on Scaling Concepts and Complex Fluids (Copanello, 1994)*; *Nuovo Cimento* D **16** 1285
[14] Hensen K, Riede W-O, Sillescu H and von Wittgenstein A 1974 *J. Chem. Phys.* **61** 4365
[15] Ivanov E N 1964 *Sov. Phys.–JETP* **18** 1041
[16] Berne B J and Pecora R 1976 *Dynamic Light Scattering* (New York: Wiley)
[17] Giordano M, Grigolini P, Leporini D and Marin P 1983 *Phys. Rev.* A **28** 2474; 1985 *Adv. Chem. Phys.* **62** 321
[18] Dries T, Fujara F, Kiebel M, Rössler E and Sillescu H 1988 *J. Chem. Phys.* **88** 2139 (Erratum 1989 **90** 7613)
[19] Hwang J S, Mason R P, Hwang L and Freed J H 1975 *J. Phys. Chem.* **79** 489
[20] Beevers M S, Crossley J, Garrington D C and Williams G 1977 *J. Chem. Soc. Faraday Trans.* II **73** 458
[21] Schlosser E and Schönhals A 1991 *Polymer* **32** 2135
[22] Ehlich D and Sillescu H 1990 *Macromolecules* **23** 1600
[23] Fan J, Marzke R F, Sanchez E and Angell C A 1994 *Proc. 2nd Int. Discussion Mtg on Relaxations in Complex Systems* ed K L Ngai, E Riande and G B Wright; *J. Non-Cryst. Solids* **172–174** 1178
[24] Dhinojwala A, Hooker J C and Torkelson J M 1994 *Proc. 2nd Int. Discussion Mtg on Relaxations in Complex Systems* ed K L Ngai, E Riande and G B Wright; *J. Non-Cryst. Solids* **172–174** 286
[25] Howell F S, Bose R A, Macedo P B and Moynihan C T 1974 *J. Phys. Chem.* **78** 639
[26] Di Schino A, Cianflone F, Andreozzi L, Giordano M and Leporini D, in preparation
[27] Rössler E, Tauchert J and Eiermann P 1994 *J. Phys. Chem.* **98** 8173
[28] Williams G and Hains P J 1972 *J. Chem. Soc. Faraday Symp.* **6** 14
[29] Shears M F and Williams G 1973 *J. Chem. Soc. Faraday Trans.* II **69** 1050
[30] Cicerone M T, Blackburn F R and Ediger M D 1995 *J. Chem. Phys.* **102** 471

[31] Saalmüller J W, Long H W, Maresch G G and Spiess H W 1996 *J. Magn. Reson.* at press
Saalmüller J W, Long H W, Volkmer T, Wiesner U, Maresch G G and Spiess H W 1996 *J. Polym. Sci.: Polym. Phys.* at press
[32] Ngai K L 1994 *Disorder Effects on Relaxational Processes* ed R Richert and A Blumen (Berlin: Springer)
[33] Schnaus W, Fujara F, Hartmann K and Sillescu H 1990 *Chem. Phys. Lett.* **166** 381
[34] Chang I, Fujara F, Geil B, Heuberger G, Mangel T and Sillescu H 1994 *Proc. 2nd Int. Discussion Mtg on Relaxations in Complex Systems* ed K L Ngai, E Riande and G B Wright; *J. Non-Cryst. Solids* **172–174** 248
[35] Lewis L J and Wahnström G 1994 *Proc. 2nd Int. Discussion Mtg on Relaxations in Complex Systems* ed K L Ngai, E Riande and G B Wright; *J. Non-Cryst. Solids* **172–174** 69
[36] Lewis L J and Wahnström G 1994 *Phys. Rev.* E **50** 3865
[37] Lewis L J and Wahnström G, private communication